Biochimica et Biophysica Acta 1838 (2014) 776–783

Contents lists available at ScienceDirect

Biochimica et Biophysica Acta

journal homepage: www.elsevier.com/locate/bbamem

Complex rhamnolipid mixture characterization and its influence on DPPC bilayer organization

E. Haba [a], A. Pinazo [b], R. Pons [b,*], L. Pérez [b], A. Manresa [a,**]

[a] Laboratorio de Microbiología, Facultad de Farmacia, Universidad de Barcelona, Joan XXIII s/n, E-08028 Barcelona, Spain
[b] Departament de Tecnologia Química i de Tensioactius, Institut de Química Avançada de Catalunya, IQAC-CSIC, Jordi Girona 18-26, E-08034 Barcelona, Spain

ARTICLE INFO

Article history:
Received 25 March 2013
Received in revised form 21 October 2013
Accepted 5 November 2013
Available online 13 November 2013

Keywords:
Biosurfactant
Rhamnolipid
Physico-chemical property
DPPC
Bilayer formation
SAXS

ABSTRACT

Rhamnolipids (RL) are one of the most important classes of biosurfactants produced by microorganisms using a wide range of carbon sources, from a simple carbon source like glucose to complex wastes such as the used cooking oils used in this work. The objective of this work was to learn about the rhamnolipid–phospholipid dipalmitoyl phosphatidyl choline (DPPC) molecular interactions through the behaviour observed in the neat products and four RL/DPPC mixtures. Size and z-potential were used to characterize the size and the charge of the vesicles, and small angle X-ray scattering (SAXS) was used to measure the vesicle bilayer characteristics, and the release of carboxyfluorescein to study the bilayer disrupting effect promoted by rhamnolipids. The results show that rhamnolipids are disposed in ordered bilayers with long repeating distances, which are stabilized by the charging of the bilayer and also by a strong fluidity of the bilayers. The ability of rhamnolipids to increase the fluidity of DPPC bilayers may be related with the strong haemolytic power of these molecules.

1. Introduction

The pressing need for more biosustainable, biocompatible and biodegradable surfactant based products makes the study of biosurfactants an important area of research. Biosurfactants are surface active biomolecules that are produced by a variety of different microorganisms [1]. Rhamnolipids (RL) produced by *Pseudomonas aeruginosa* are a mixture of mono-rhamnolipids and di-rhamnolipids. Mono-rhamnolipids consist of one rhamnose molecule (Rha) linked to one or two molecules of hydroxy acid of different chain lengths [2]. Di-rhamnolipids consist of two Rha molecules linked to one or two molecules of hydroxy acid. The structure of mono- and di-rhamnolipids is shown in Fig. 1.

Rhamnolipids have the two main properties of surfactants, that is, strong surface activity and self-assembly in water [3]. The advantages of these surfactants, as compared with the synthetic ones, are low toxicity, high biodegradability and ecological safety. Rhamnolipids self-assemble to form micelles, vesicles and bilayers. The vesicles contain one or more surfactant bilayers surrounding an aqueous core [4,5]. Therefore, they can encapsulate either water-soluble compounds in their inner aqueous phase or oil-soluble substances in their outer bilayer region, resulting in their potential use as a vehicle, or carrier, for active ingredients in cosmetics and pharmaceutical applications [6]. Vesicles can be obtained in different surfactant systems, such as single surfactant dispersion, surfactant mixtures or with the addition of a co-solute into the surfactant solution.

Despite the importance the interaction between rhamnolipids and membranes might play in their biological mechanism of action, very little is known, especially regarding rhamnolipid–phospholipid molecular interactions. In the present work, the behaviour of a complex mixture of rhamnolipids (RL8) and its combination with a phospholipid, dipalmitoyl phosphatidyl choline (DPPC), are studied to fill this gap and explore the potential use of rhamnolipids in the cosmetics fields in which compound biocompatibility is important. The interactions have been evaluated by investigation of the size and charge of the vesicles as well as by determining the bilayer characteristics. The fact that RL8 is produced from residual frying oil and used as a whole mixture makes the process more economically attractive as we deal with an added value product. Finally, with the desire to open new fields for rhamnolipids in new applications a preliminary screening of biocompatibility of the RL8/DPPC formulations with red blood cells is presented.

2. Material and methods

2.1. Materials

1,2,Dipalmitoyl-sn-glycero-3-phosphocholine (DPPC) was purchased from Sigma-Aldrich Chemical Co. Aqueous dispersions were prepared with Pure Millipore water from a Milli-Q four-bowl system. 5(6)-

* Correspondence to: R. Pons, Departament de Tecnologia Química i de Tensioactius, Institut de Química Avançada de Catalunya, IQAC-CSIC, Jordi Girona 18-26, E-08034 Barcelona, Spain. Tel.: +34 934006150.
** Correspondence to: A. Manresa, Laboratorio de Microbiología, Facultad de Farmacía, Universidad de Barcelona, Joan XXIII s/n, E-08028 Barcelona, Spain.
E-mail addresses: ramon.pons@iqac.csic.es (R. Pons), amanresa@ub.edu (A. Manresa).

0005-2736/$ – see front matter © 2013 Elsevier B.V. All rights reserved.
http://dx.doi.org/10.1016/j.bbamem.2013.11.004

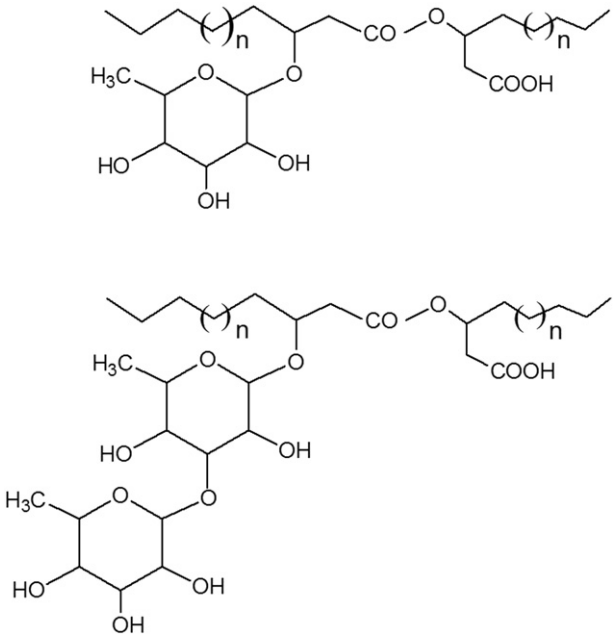

Fig. 1. Molecular structure of mono- and di-rhamnolipids. N = 4, 6 or 8.

Carboxyfluorescein (CF) was obtained from Fluka. Sephadex G-50 was from General Electric. Tris(hydroxymethyl)-aminomethane was from Merck and was used to prepare Tris–HCl buffer at a concentration of 20 mM at pH = 7.4. Triton X-100 was from USB.

2.2. Micro-organisms and growth culture

Due to its capacity to produce surface-active rhamnolipids from hydrophobic substrates *P. aeruginosa* 47T2 NCIB 40044 was selected. After being grown on TSA (Trypticase Soy Agar, Pronadisa, Barcelona, Spain), the bacterial strain was maintained at 4 °C and was also preserved in cryobilles (AEB 400100 EAS Laboratoire, France) at −20 °C.

Experiments were carried out in 2 l baffled Erlenmeyer flasks containing 400 ml of medium with the following composition (g/l): $NaNO_3$ 5, KH_2PO_4 2.0, K_2HPO_4 1.0, KCl 0.1, $MgSO_47H_2O$ 0.5, $CaCl_2$ 0.01, $FeSO_47H_2O$ 0.012 and yeast extract 0.01. 0.05 ml of a trace element solution containing (g/l): H_3BO_3 0.26, $CuSO_4 \cdot 5H_2O$ 0.5, $MnSO_4 \cdot H_2O$ 0.5, $MoNa_2O_4 \cdot 2H_2O$ 0.06 and $ZnSO4 \cdot 7H_2O$ 0.7, was added. Finally, 40 g/l of olive/sunflower (50:50; v/v) waste frying oil was used as carbon source containing oleic acid (50.29%) and linoleic acid (34.23%) as major components and stearic acid (7.70%) and palmitic acid (7.77%) in small quantities.

Medium components were sterilized separately at 120 °C, 1 atm for 20 min. The initial pH of the medium was adjusted to 7.2. A 2% (v/v) cell suspension in sterile saline (0.9% NaCl) of an overnight culture on TSA (Pronadisa, Barcelona, Spain) was used as inoculum. Cultures were incubated at 30 °C on a reciprocal rotary shaker at 150 rpm.

2.3. Rhamnolipid production and characterization

Rhamnolipids were recovered and purified: Cells were removed from the culture by centrifugation (12,000 ×*g*) for 30 min. Purification was achieved by adsorption chromatography on a polystyrene resin Amberlite XAD2 (Supelco, USA). The resin (60 g) was placed in a glass column (60 × 3 cm), yielding a bed volume of 200 ml. The column was equilibrated with 0.1 M phosphate buffer, pH 6.1. The culture supernatant was applied through a sieve placed on top of the resin. The adsorption of the active compounds on the resin was monitored by measuring the surface tension (γ_{ST}) of the column outlet. The saturation of the resin was terminated when γ_{ST} of the effluent dropped below 40 mN/m. Then the column was washed with three volumes of distilled water. Biosurfactants were eluted with methanol and finally the solvent was evaporated to dryness under vacuum (Büchi, Flawil, Switzerland).

LC–MS was performed to check the purity of the extract, indicated by the absence of residual fatty acids. To analyze the composition of the RL mixture, a 10 mg portion was resuspended in 1 ml of methanol and analyzed by HPLC–MS. Rhamnolipid mixtures were separated and identified by liquid chromatography coupled to mass spectrometry using a Waters 2690 separation module (Waters, Milford, MA). The samples were injected (10 μl) into a Spherisorb ODS2 C_{18} with a 150 · 4.6 mm column (Teknokroma, Sant Cugat, Spain). The LC flow-rate was 1 ml/min. An acetonitrile-water gradient was used starting with 30% acetonitrile for 2 min followed by a ramp of 30–100% acetonitrile for 30 min, left to stand for 5 min and then returned to initial conditions. Post-column addition of acetone at 200 μl/min was performed using a Phoenix 20 (Carlo Erba, Italy) because an enhancement of sensitivity to rhamnolipids was observed. The LC effluent and acetone were mixed in a tee valve (Valco) and split (1/50) before entering the mass spectrometer. MS was performed with a single quadrupole mass spectrometer, VG Platform II (Micromass, Manchester, UK), equipped with a pneumatically assisted electrospray (ES) source. The negative ion mode was used (N-ES). Full scan data were obtained by scanning from m/z 100 to 750 in the centroid mode using scan duration of 2.0 s and an inter-scan time of 0.2 s. The working conditions for N-ES were as follows: dry nitrogen was heated to 80 °C and introduced into the capillary region at a flow-rate of 400 l/h. The capillary was held at a potential of −3.5 kV and the extraction voltage was held at −80 V. Rhamnolipid homologues were quantified from the molecular proportion of each of the pseudomolecular ions calculated by LC–MS.

2.4. Qualitative phase behaviour

Optical microscopy was employed to study the phase behaviour of binary RL8/water system. Optical observations were performed according to the "flooding" (penetration) method of Lawrence [7]. A Reicher Polyvar 2 Leica polarizing microscope equipped with a hot stage was employed. A camcorder and a PC with Leica IM 500 software were used to capture images. In a flooding experiment, water was allowed to diffuse into an anhydrous surfactant placed between a slide and a cover slip. After a short time, gradients in composition were produced and different separated mesophases developed around the crystalline surfactant.

2.5. Vesicle preparation

Rhamnolipid vesicles were prepared following Bangham method [8]. We start from 5 ml of a chloroform solution containing 0.6% of RL8. The solvent was evaporated under vacuum until dry. The obtained film was hydrated with 5 ml of Milli-Q water and agitated until total dispersion. Then it was sonicated for 15 min at 30 °C. Vesicles were formed with 600 mg/l, 800 mg/l, 1100 mg/l and 1400 mg/l RL8 contents.

Vesicles that were formed with a mixture of RL8 and DPPC were prepared following the method just described but at 40 °C. The desired amount of DPPC was dissolved in chloroform and then evaporated until dried. The obtained film was hydrated to obtain the desired concentration. RL8 aqueous dispersion was prepared separately weighing the convenient amount of compound and dissolving in water. Before mixing, the two aqueous dispersions were strongly stirred for 10 min to obtain vesicle dispersions. Then dispersions were mixed and sonicated for 15 min at 40 °C. In the case of RL8/DPPC 60/40, mixed vesicles were also prepared by forming a mixed film and posterior hydration and sonication. Those vesicles produced SAXS patterns identical to the previous ones within the experimental error.

We applied the method described above for the preparation of DPPC at pH = 5. The pH was adjusted by adding small amounts of 0.1 M HCl solution up to a pH of 5.

2.6. Size and zeta potential

Size and zeta potential of vesicles were obtained by analyzing the samples in a Zetasizer Malvern Nano-ZS using a ZeNO112 cell. The value was taken as the mean of three independent measurements. Each measurement is in turn the average of ten sub-measurements of 20 s each.

2.7. Small angle X-ray scattering

Small angle X-ray scattering (SAXS) was performed using a S3-MICRO (Hecus X-ray systems GMBH, Graz, Austria) coupled to a GENIX-Fox 3D X-ray source (Xenox, Grenoble) which produces a detector-focused X-ray beam with λ = 0.1542 nm Cu Kα-line at greater than 97% purity and less than 0.3%Kα. The transmitted scattering was detected using a PSD 50 Hecus at small-angle regime ($0.09\ nm^{-1} < q < 6\ nm^{-1}$). Temperature was controlled through a Peltier TCCS-3 Hecus. The samples were inserted in a flow-through glass capillary with 1 mm diameter and 20 μm wall thickness. The SAXS curves are plotted as a function of the scattering vector modulus, $q = 4\pi / \lambda \sin(\theta / 2)$, where θ is the scattering angle and λ the wavelength of the incident radiation. The system scattering vector was calibrated by measuring a standard silver behenate sample. Scattering curves were primarily smeared by the detector width because we used a detector-focused small beam (300 × 400 μm full width at half maximum), which widens the peaks without a noticeable effect on peak position. The background was subtracted to the scattering curves. These curves were scaled in absolute units by comparison with water scattering [9,10]. The instrumentally smeared experimental SAXS curves were fitted to numerically smeared models for beam size and detector width effects [11]. A least squares routine based on the Levenberg–Marquardt scheme was used. The bilayer was fitted using a three-Gaussian profile based on the MCG model following Pabst et al. [12,13].

Specifically the bilayer is calculated as a summation of the headgroup contribution (in the form of a Gaussian centred at $\pm Z_h$, amplitude σ_h and maximum electron density ρ_h), the methyl groups contribution (in the form of a Gaussian centred at 0 with amplitude σ_c and maximum electron density ρ_c). In addition to these two contributions and, as a difference with the original model of Pabst et al. [12] a third contribution corresponding to a step function centred at the bilayer centre, width 2 and electron density contribution $(\rho_{CH_2} - \rho_{H_2O})$ corresponding to the difference in electron density between the bilayer methylene and the outer water. The unidimensional Fourier transform of the headgroup contribution corresponds to Eq. (1), that of the methylene groups to Eq. (2) and the global one including that of the step function to Eq. (3). The structure is modeled according to the modified Caillé model as in Pabst et al. [12] (Eq. (4)) and the global intensity is calculated according to Eq. (5), where N_{diff} corresponds to a fraction of uncorrelated bilayers.

$$F_h(q) = \sqrt{2\ \pi}\ \sigma_h\ \rho_h \exp\left(-\sigma_h^2\ q^2/2\right)\ cos(qZ_h) \tag{1}$$

$$F_c(q) = \sqrt{2\ \pi}\ \sigma_c\ \rho_c \exp\left(-\sigma_c^2\ q^2/2\right) \tag{2}$$

$$F(q) = 2F_h(q) + F_c(q) + \left(\rho_{CH_2} - \rho_{H_2O}\right) \sin(Z_h q)/q \tag{3}$$

$$S(q) = N + 2\sum_{k=1}^{N-1} (N-k) \cos(kqd)\, e^{-(d/2\pi)^2 q^2 \eta_1} \gamma (\pi k)^{-(d/2\pi)^2 q^2 \eta_1} \tag{4}$$

$$I(q) = \left| F(q)^2 S(q) + N_{diff} F(q)^2 \right| / q^2. \tag{5}$$

The parameters in Eq. (4) correspond to *N*, total number of correlated bilayers, *d* repetition distance, η_1 the Caillé parameter and γ to the Euler constant.

The bilayer term in Eq. (3), absent in the original model, is particularly useful for fitting bilayers with a thick water layer, which produces an asymmetric electron density distribution around the headgroup.

2.8. Haemolytic activity

The haemolytic activity was analyzed following the method published by Zaragoza et al. [14]. Human erythrocytes were prepared right before the experiments from red blood cell concentrates. Cells were washed four times with buffer (150 mM NaCl, 5 mM HEPES at pH 7.4), and finally suspended in the same volume of buffer prior to use. All operations were carried out at 4 °C.

Haemoglobin release was determined, upon incubation of red blood cells with di-rhamnolipid under different conditions by measuring the absorbance at 540 nm after pelleting the membranes by centrifugation for 2 min. Temperature was maintained constant at 37 °C. The total amount of haemoglobin was established by lysing the erythrocytes with distilled water, and the value obtained was taken as 100% of haemoglobin release.

2.9. Carboxymethylfluorescein entrapment and release

100 mM CF solution was prepared in Tris–HCl 20 mM, 300 mM NaCl at pH 7.4. CF was encapsulated following the method described by Weinstein et al. [15]. Vesicles were prepared according to the protocol described in Section 2.5. Hydration of either DPPC or RL/DPPC mixtures (20/80, 40/60, 60/40 and 80/20) (25 mg/ml) was performed with 1 ml of Tris–HCl 20 mM buffer solution (pH 7.4) plus 1 ml of CF 100 mM. The suspension was mixed by vortexing for several minutes and then sonicated for 15 min. Free CF was removed from vesicular suspension by gel filtration through a Sephadex G-50 column equilibrated with Tris–HCl 20 mM (pH 7.4) eluting in Tris–HCl 20 mM, 100 mM NaCl (pH 7.4).

Release studies were carried out in ice-cold Tris–HCl (pH 7.4) over a 30 min period time or until the value of measured intensity was constant. An aliquot of 0.5 ml CF-loaded vesicles was taken in a fluorescence cuvette and diluted with the release medium resulting in a final volume of 3 ml. Fluorescence measurements at 25 °C were performed on a Shimadzu RF-540 spectrofluorophotometer using an excitation wavelength of 495 nm and emission of 515.4 nm. The total amount of CF encapsulated was determined by adding 60 μl of Triton X-100 10% (v/v) aqueous solution to 3 ml of vesicle dispersion.

3. Results and discussion

3.1. Rhamnolipid RL8 production and chemical characterization

Rhamnolipids are accumulated in the culture as a mixture of different homologues, and the final composition of the mixture depends on the bacterial strain and the substrate composition. The most commonly used method for biosurfactant recovery in rhamnolipid production is acid precipitation prior to purification; in the case under study as the substrate is a mixture of waste frying oils, other fatty acid components from the culture supernatant might contaminate the desired product. Adsorption column chromatography proved to be a simple technique for purifying rhamnolipid mixtures from the culture. After saturation, monitoring and elution, the recovery yield was 61%. The degree of purification was monitored by LC. No free fatty acids were detected in the isolated product. After total methanol evaporation, rhamnolipids look like sticky, semi-solid, brown-coloured oil with a characteristic smell.

The composition of the surfactant produced was determined by LC–MS–ES. The surfactant was produced by *P. aeruginosa* 47T2 after 96 h of incubation and was composed of 8 homologues (RL8), in which the proportion of each component was calculated from the areas obtained for each molecule of RL by LC–MS. As shown in Table 1, 60.4% were mono-rhamnolipids: Rha-C_8-C_{10}; Rha-C_{10}-C_{10}; Rha-C_{10}-C_{12}; Rha-C_{10}-$C_{12:1}$ and 39.6% were di-rhamnolipids: Rha-Rha-C_8-C_{10}; Rha-Rha-C_{10}-C_{10}; Rha-Rha-C_{10}-C_{12} and Rha-Rha-C_{10}-$C_{12:1}$.

It is known that the properties of rhamnolipids depend on the distribution of their homologues, but little is known about the contribution of each individual homologue to the surface properties of rhamnolipid mixtures thereby the di-rhamnolipid Rha-Rha-C_{10}-C_{10} showed a CMC value of 110 mg/l while two different mixtures mainly containing mono-rhamnolipids, M6 and M7, showed CMC values of 230 and 150 mg/ml respectively [16]. The more hydrophilic rhamnolipids Rha-C_{10} and Rha-Rha-C_{10} showed CMC values of 200 mg/l [17].

The new surfactant (RL8) decreased the surface tension of water from 72.0 mN/m to 32.21 mN/m and the CMC was 105 mg/l. This value, although slightly lower than that found with a rhamnolipid mixture of 11 homologues (108 mg/l) produced by the same strain [18], should be considered coincident from a statistical viewpoint. This little difference may be due to the lower amount of unsaturated components of the surfactant produced in the present study, 9.9%, compared with that (13.9%) reported by Haba et al. [18]. The effect of the presence of unsaturated compound was also reflected as well in the case of strain LBI containing up to 31% of unsaturated carbon, with a CMC of 120 mg/l [19] or in the case of the AT10 strain with a CMC of 150 mg/l and up to 43.2% of unsaturated compounds [16].

3.2. Qualitative phase behaviour

RL8 qualitative aqueous phase behaviour was studied by the Lawrence method [7] that is, observing how water penetrates a sample of dry material on a glass slide at 25 °C. After several minutes, a concentration gradient develops (Fig. 2), and two distinctive areas of birefringence are visible with a mosaic texture typical of lamellar phases (Fig. 2 top, see arrow) separated from a myelin structure (Fig. 2 bottom, see arrow). Myelin may be considered as intermediate structures formed during the transformation of surfactants into hydrated bilayers [20]. In RL8 myelin shapes coexist both with concentric and rod-like bilayer arrangements which alternate with water pockets. This complex self-assembly appears especially stable and reproducible.

3.3. Size and zeta potential

Vesicle size, size distribution, and charge density are important parameters in vesicle applications. In order to observe the effect of formulation on these parameters we studied the following compositions: RL8, DPPC and mixed RL8/DPPC at four different molar ratios (80/20, 60/40, 40/60, 20/80) all of them at 1400 mg/l. All formulations were characterized by Dynamic Light Scattering (DLS) to determine vesicle size and size distribution.

RL8 are weak acids with pKa ranging from 4.28 to 5.50 depending on the concentration [21]. Thus, mixtures of RL8 and DPPC are slightly acidic. DPPC vesicle size was measured at pH 5 in order to have coherent results. For the low concentration samples used in these determinations, the proportion of mono- and di-rhamnolipids in the bilayer is not very far from that of the bulk. According to the results of Chen et al. [22], for a mixture of 60% mole fraction of R1 (close to ours) the composition of the adsorbed layer at the air–water interface is only slightly enriched in R1. As these results were obtained at pH 9, where the difference in behaviour between R1 and R2 is the biggest, we do not expect significant differences in the composition of the bilayers and the bulk composition of the rhamnolipids.

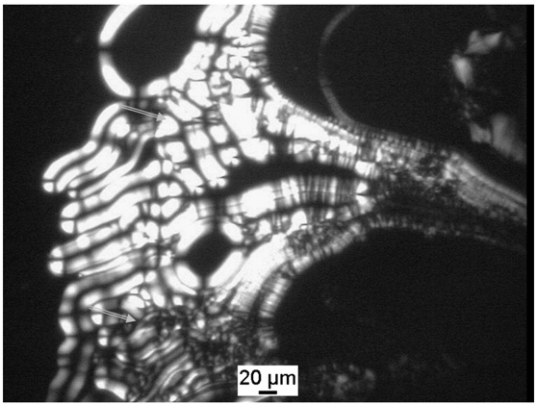

Fig. 2. Cross polarized light microscopy image of water penetration experiment in dry RL8 at 25 °C taken after 10 min of interaction.

Fig. 3 shows the intensity distribution as a function of size. In all cases scattering detected two noticeable ranges of sizes corresponding to medium and large vesicles respectively. For DPPC dispersions (Fig. 3a) vesicle sizes ranged from 60 to 80 nm and from 350 to 400 nm. This result is fairly consistent with the results reported by Kim et al. [23].

For rhamnolipid solutions, the average vesicle sizes are slightly bigger than for DPPC; however, they remain fairly within the same ranges, 80–150 nm and 300–700 nm (Fig. 3f). These results agree with those reported by Sanchez et al. [2] for purified di-rhamnolipids. Pornsuthorntawee et al. [24] described bimodal distribution of aggregate sizes for RL concentrations above 200 mg/l that above RL concentrations of 1200 mg/l become monomodal due to disappearance of the medium size vesicles. However, a bimodal population was found by our group at concentrations as high as 1400 mg/l.

For RL8/DPPC mixtures, increasing the amount of DPPC resulted in broader size distribution favouring formation of vesicles with growing sizes (Fig. 3b, c). As the size distribution broadens, the maximum scattered intensity decreases. There is a consistent displacement of the mean size of the population as the proportion of RL8 increases. Some of this displacement can be rationalized based on the different amphiphilic behaviours of DPPC and RL8 and taking also into account the different scattering powers of different sized particles. We have to take into account that the bigger sizes have higher scattering power and may correspond to a small number of particles. Thus, the smaller size component in d, e and f may correspond to populations of

Table 1
Components of RL8 mixture produced by *P. aeruginosa* 47T2 using frying oil as carbon source in a submerged aerate culture at 30 °C after 96 h of incubation.

RL8 components	Pseudo-molecular ion (m/z)	Relative abundance (%)	Fragments (m/z)
Rha-C_{10}-C_{10}	503	39.1	333, 169, 119, 103
Rha-Rha-C_{10}-C_{10}	649	19.7	479, 169, 163
Rha-Rha-C_{10}-C_{12}/Rha-Rha-C_{12}-C_{10}	677	10.7	507, 479, 197, 169, 163
Rha-C_{10}-C_{12}/Rha-C_{12}-C_{10}	531	8.4	361, 333,169, 163, 119, 103
Rha-C_{10}-$C_{12:1}$/Rha-$C_{12:1}$-C_{10}	529	9.9	333, 197, 169, 163, 119, 103
Rha-Rha-C_{10}-$C_{12:1}$	675	6.3	479, 195, 169, 103
Rha-Rha-C_8-C_{10}	621	2.9	451, 169, 141
Rha-C_{10}-C_8/Rha-C_8-C_{10}	475	3.0	305, 169, 163, 141, 119,103

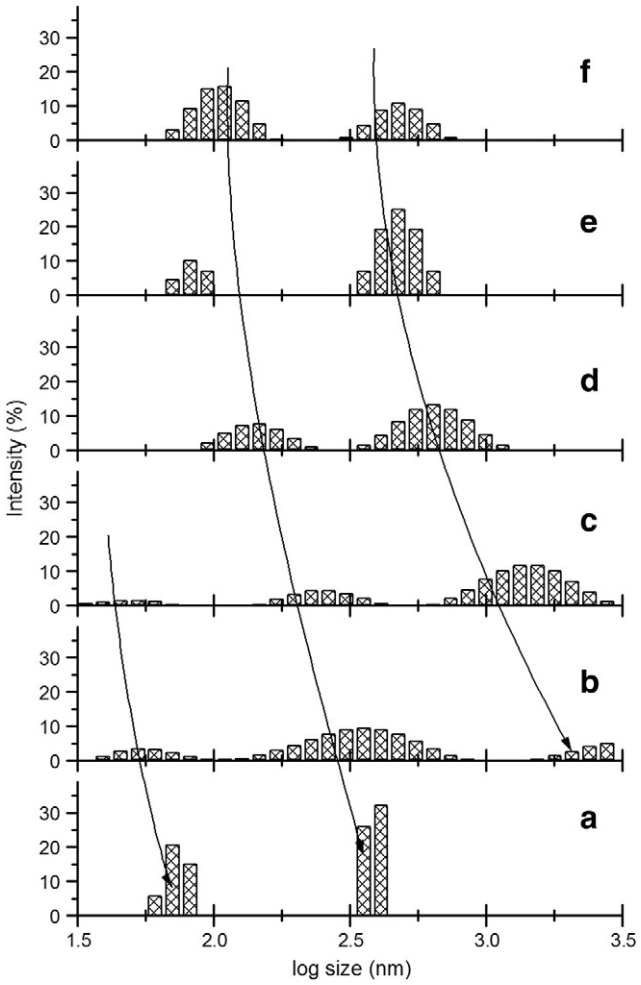

Fig. 3. Scattered intensity particle size distributions of 1400 mg/l aqueous dispersions of RL8/DPPC mixtures as obtained from DLS at 25 °C. Size axis is given in logarithmic scale. a) 0/100 RL8/DPPC (DPPC in acidic media), b) 20/80 RL8/DPPC, c) 40/60 RL8/DPPC, d) 60/40 RL8/DPPC, e) 80/20 RL8/DPPC, and f) 100/0 RL8/DPPC.

spontaneous vesicles mainly originated from RL8. This situation differs from the solubilization of liposomes by single-chain synthetic surfactants where the size of the liposomes remains essentially unchanged while the presence of mixed micelles is appreciated at small sizes [25].

The zeta-potential is obtained from the measurement of the electrophoretic mobility and is related to the electric charge of the vesicles [26]. As a rule of thumb, it is considered that a system is electrostatically stable if the zeta-potential has an absolute value above 20 mV.

The DPPC molecule has a hydrophilic part with a negative charge on the phosphate group and a positive charge on the choline group and, therefore, DPPC should be neutral overall. However, the DPPC vesicles show a zeta-potential of 60 mV, that is, they support a positive electric charge. A rational for this behaviour is that, in an acid solution, the phosphate group is partially neutralized by protons whereas the choline group remains positively charged. This is quite different from the neutral pH conditions where the DPPC vesicles have a slightly negative charge (~−20 mV) or slightly positive charge depending on ionic strength [27].

Negative zeta-potential values have been obtained for all the mixtures studied (see Fig.4). The addition of amphoteric phospholipids to rhamnolipid does not have a noticeable effect on the zeta-potential of the aggregates. The large difference between the z-potential of the acidic DPPC and the mixtures with rhamnolipids is a bit surprising. This could be related to the pKa effects found in membranes when mixing

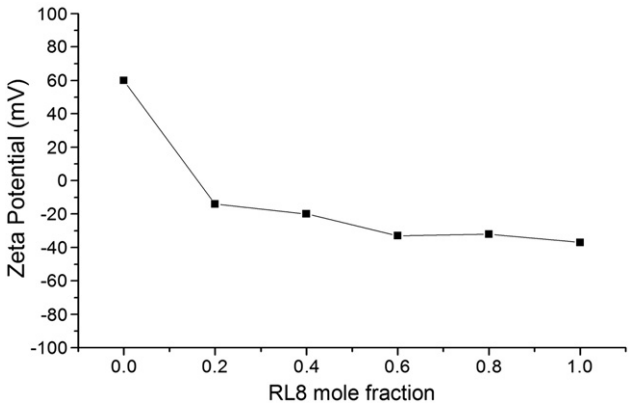

Fig. 4. Mean zeta-potential of RL/DPPC mixtures as a function of RL8 mole fraction at 1400 mg/l.

zwitterionic and anionic phospholipids [28]; however, this point is out of the scope of this article.

3.4. Bilayer microstructure in mixtures of RL8 surfactants and phospholipids

3.4.1. Binary systems of RL8 in water

It has been described that, at high concentrations, mono-rhamnolipids have predominantly planar structures (unilamellar or bilamellar vesicles), whereas, di-rhamnolipids form globular aggregates [3,22,29]. Mixtures of mono and di-rhamnolipids show the transition from globular to lamellar aggregates at moderate concentrations (between 3 and 6% in weight at pH 9) [22]; the evidence of planar aggregates is found at smaller concentrations (2%) at acidic pH [30]. In this context, we aim to determine the type of structures that form the complex mixture of rhamnolipids RL8. RL8 surfactant in water was studied at different concentrations of 6%, 8%, 11% and 14% w/w. Small angle X-ray scattering (SAXS) provides information on the structural features of the sample in the range of 0.5 to 50 nm. In Fig. 5 the SAXS patterns obtained at 25 °C, together with the fit of a bilayer model are presented. The model used here is a modification of the MCG model [12,13]. The four concentrations can be fitted to lamellar structures, which means that the RL8 molecules are arranged in layers with defined periodicity. The curve profiles present small differences at small q values, with increasing intensity when increasing concentration and the appearance of a shoulder at q values around 0.1–0.2 nm^{-1} and a broad peak compatible with bilayers

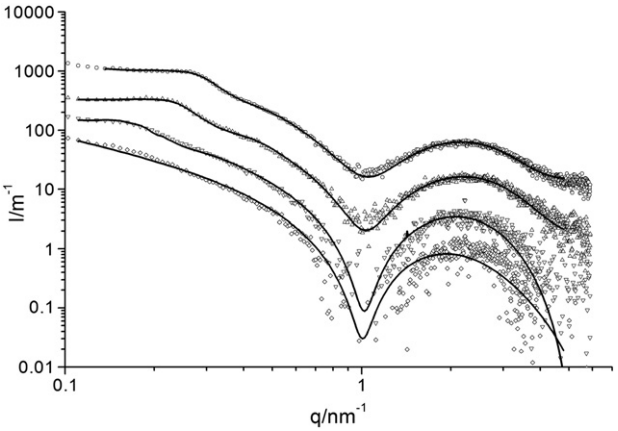

Fig. 5. Small X-ray scattering intensity patterns recorded at 25 °C for RL8/H_2O systems, diamonds 600 mg/l, down triangles 800 mg/l, up triangles 1100 mg/l, circles 1400 mg/l and best fit of the MCG model (lines) to the diffraction pattern. The curves have been multiplied by increasing factors of 2, and the absolute scale corresponds to the sample of 6%.

at q values around 2 nm^{-1}. No significant differences are observed in this region of the scattering curves.

The fit of the MCG model to the experimental points is good over the entire q range. The bilayer thickness (d_b) was directly determined from the fitting parameters using the following equation.

$$d_b = 2\ (Z_H + \sigma(FWHM)_H/2)$$

where Z_H and $\sigma(FWHM)_H$ are the centre and full width at half maximum, respectively, for the head group Gaussians [13]. The repetition distance of the lamellar structure, d, obtained for the systems 14%, 11% and 8% is 21.4 nm, 25.5 nm and 35.0 nm respectively. The sample with 6% did not show, within the accessible range, the presence of a repetition distance. The high degree of dilution that can be achieved with these bilayers is remarkable. There are not significant differences in the obtained electronic density profiles for the bilayers (only the 6% sample may deviate but is also the one subjected to the smaller signal-to-noise ratio, see Fig. 6).

The bilayer thickness obtained from the fit or from the relation $d_B = d * \varphi$, where φ is the volume fraction, coincides in values of 2.7 ± 0.2 nm. The electronic profiles show the presence of big polar heads combined with small hydrophobic tails. This implies that there should be a significant interpenetration of what can be considered the hydrophilic and hydrophobic moieties because the low electronic density region has electronic densities sensibly similar to that of water. Also, the hydrophobic moieties need to be interdigitated because of the small hydrophobic thickness. Taking into account the results described above we propose a low resolution model for the RL8 bilayer (Fig. 7). The distance between the bilayers is considerable and can accommodate a huge amount of water molecules. The model only represents the two major RL present in the RL8 mixture.

3.4.2. RL8/DPPC/water ternary systems

We explore the effect of mixing the rhamnolipid with a phospholipid in the bilayer characteristics. As it can be observed in Fig. 8, the fit of the MGG model to the experimental scattering patterns is good over the entire q range. The structural parameters generated from fits for the four mixed systems and, single RL8 and DPPC in water and in water at pH 5 and are listed in Table 2.

The fits correspond to lamellar structures with repetition distance $d = 21.4$ nm for pure RL8 aqueous dispersions and $d = 6.3$ for DPPC dispersions. Dispersions of DPPC in acidic water (at a pH = 5.8 which corresponds to the pH produced by 14% of RL8) did not show evidence of ordering, in this case a single bilayer can be fitted with a bilayer thickness $d_b = 4.8$ nm. Using the relation $\varphi = d_b/d$, we can calculate the volume fraction corresponding to the material that is producing this

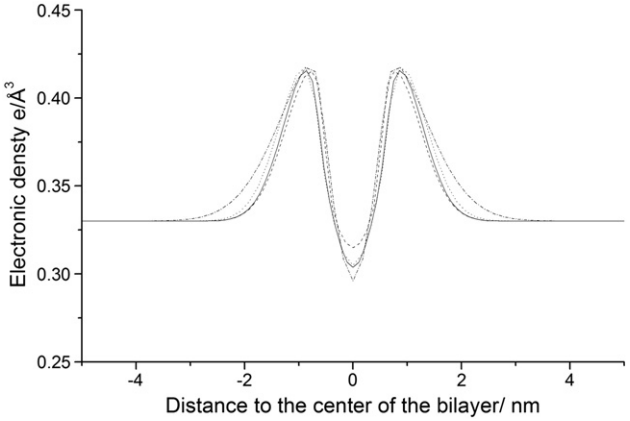

Fig. 6. Electronic density profile across the bilayer for samples of 600 mg/l (dot-dash), 800 mg/l (dots), 1100 mg/l (dash), and 1400 mg/l (full line) (the same concentrations corresponding to Fig. 5) as obtained from the SAXS fits.

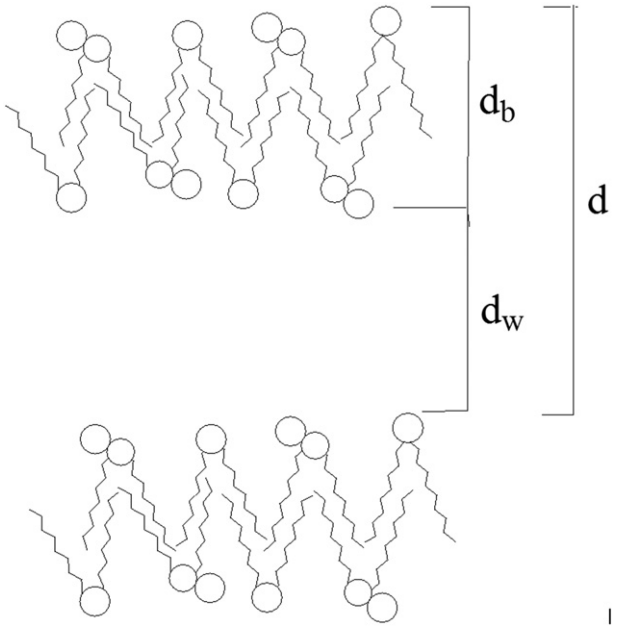

Fig. 7. Sketch of RL8 bilayer in water. d, bilayer repetition distance. d_b, bilayer thickness and d_w, water thickness.

repetition distance. This corresponds to 0.12, 0.10, 0.11, 0.25, 0.24 and 0.59 going from RL8 to the DPPC in aqueous media (obviating the acidic DPPC which would result in null volume fraction). Based on these results we can say that the RL8 dispersion and the two first mixtures correspond to very swollen lamellar liquid crystalline phase while for the samples where the phospholipid predominates, the lamellar phase does not occupy the entire volume and there is excess water present in the system. The ability of the RL8 to swell the DPPC liquid crystalline phase is probably related to the bilayer charging effect combined with higher bilayer fluidity. Using the bilayer fraction of the lamellar phase we can calculate the mean area per molecule in this phase. The area per molecule obtained for the pure RL8 is 0.63 ± 0.02 nm^2 and 0.65 ± 0.02 nm^2 for DPPC. The mean area per molecule of the mixtures is systematically smaller than that of the pure systems (i.e. 0.49, 0.54, 0.62 and 0.57 nm^2 in order of increasing DPPC content). The shrinkage observed for the 80/20 RL8/DDPC mixture which indicates a strong compatibility for the bidimensional solution of DPPC molecules in a RL8 layer is especially remarkable. The presence of RL8 molecules

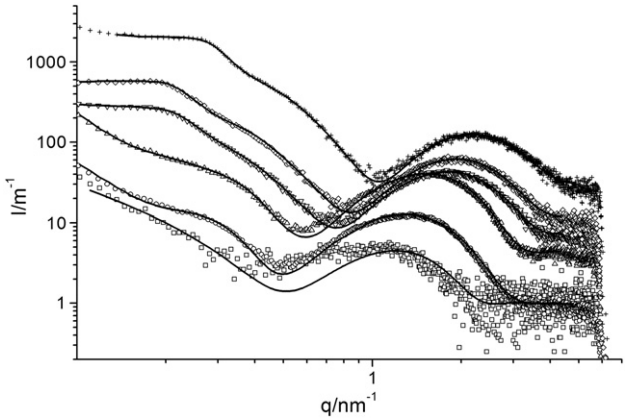

Fig. 8. Small X-ray scattering intensity at 25 °C for RL8/DPPC/H_2O systems at constant lipid weight content of 1400 mg/l. DPPC at pH 5.8 squares, 20/80 RL8/DPPC circles, 40/60 up triangles, 60/40 down triangles, 80/20 diamonds, RL8 crosses. Best fit of the MGG model (lines). The curves have been multiplied by increasing factors of 2, and the scale corresponds to the DPPC sample.

Table 2
Parameters of the fits of the SAXS patterns for mixtures RL8/DPPC in different proportions and acidic DPPC at 25 °C.

Parameters[a]	100/0	80/20	60/40	40/60	20/80	DPPC-H$^+$	DPPC[c]
d (nm)	21.4	28.8	27.6	14.2	16.8	–	6.3
η_1	0.59	0.54	0.80	1.28	0.19	–	0.0009
N	5.5	124	78	2.6	1.6	–	33
σ_h (nm)	0.54	0.49	0.50	0.56	0.80	0.58	0.14
σ_c (nm)	0.63	0.72	0.70	0.76	0.50	1.15	0.80
ρ_h (e/nm^3) × 10^{-3}	0.47	0.50	0.50	0.50	0.45	0.60	0.64
ρ_c (e/nm^3) × 10^{-3}	0.21	0.24	0.24	0.24	0.19	0.25 [b]	0.25
Z_H (nm)	0.63	0.88	0.95	1.13	1.10	1.71[b]	1.71
d_b (nm)	2.5	2.9	3.1	3.6	4.1	4.8	3.75

[a] d bilayer repetition distance, η_1 Caillé parameter, N number of correlated bilayers, σ_h and ρ_h head group width and electron density, σ_c and ρ_c methyl width and electron density, Z_H head group-head group distance and d_b bilayer thickness.
[b] The scattering curves were very noisy, so no peaks were apparent and the fitting was restricted using the same values of DPPC for the marked parameters.
[c] Scattering pattern not shown in Fig. 6.

maintains the DPPC bilayer in the fluid phase. This behaviour was also observed for the gel–liquid crystalline transition of phospholipids with purified di-rhamnolipid as observed from the hydrocarbon chain conformation [31]. This behaviour is consistent with the known behaviour of mixtures of sugar and phospholipids [32] where the sugar reduces the transition temperature of the phospholipid. Moreover, the Caillé parameter (η_1), which is related to membrane elasticity (the higher the value of η_1 lower the membrane elastic modulus) has the lowest values for DPPC and for the mixture 20/80 which indicates high rigidity of these membranes compared with the mixtures and the pure RL8 membranes. However, we should be cautious when using the values of Caillé parameter and number of correlated lamellae for these samples due to the wide water layer present, which makes the repeating distances very long, and the correlation peaks little defined. Polar groups are one of the structural factors that affect the molecular packing in mixed monolayers. Their nature, orientation, mutual interaction and degree of hydration are crucial for the molecular packing [33].

Assuming that the influence of the electric charge is essentially limited to the head group, the comparison between the η values for RL8/DPPC mixtures shows that it is the anionic group in the rhamnolipid molecule which has an influence on the elasticity of DPPC bilayer. This influence depends not only on the anionic charge but also on the charge density of the chemical group involved, on their extent of binding and, on the smallest distance from the cationic charge to the positive end of the DPPC dipole [34]. Also, there is an influence of mixing on the reduction of the rigidity for the intermediate mixtures.

The bilayer thickness, that is, the non aqueous portion of the lamellar phase, increases as the content of DPPC increases. In this case, the sample comparable with the rest is that of the DPPC in acidified media. This increase is reasonable in terms of the size of the hydrophobic chains of the molecules and in terms of the size of the polar heads which show little dependence on the composition except considering the DPPC in neutral media.

3.5. Haemolytic activity

Haemolysis by surfactants is a process of great fundamental and practical importance. The mammalian erythrocyte lacks internal organelles, and since it is the simplest cellular model obtainable, it is the most popular cell membrane system to study the surfactant–membrane interaction [35].

Since the haemolytic activity of pure di-rhamnolipids has been already described [36], the aim of this study was to screen if the combination of RL8 and DPPC had the same effect described before on red blood cells or the presence of phospholipid would be able to reduce the haemolytic action of the surfactant. Thus, the RL8 and RL8/DPPC mixtures used above (80/20, 60/40, 40/60 and 20/80 at 0.14% w/w) were contacted with human red cells, to observe their interaction. The release of haemoglobin was measured in a discontinuous assay at 37 °C, because of the need to pellet down the cells in order to quantify the amount of haemoglobin released. One hundred percent haemoglobin release was determined after lysing the cells with distilled water.

The degree of haemolysis induced by the RL8/DPPC formulations is shown in Fig. 9. A strong haemolytic activity in all of the samples was obtained. When DPPC was present in the sample, haemolysis was found to be a little lower than that of the corresponding RL8 alone. When different dilutions were made (1:10, 1:100 and 1:1000) it could be observed that, in the formulations where DPPC was over 50%, there was a significant decrease in haemolysis while, the combinations where DPPC is the minor component, dilution 1:1000 exhibits a 60% reduction of the haemolytic activity.

Recently the action of rhamnolipids on biological membranes [14] has been studied. The authors establish that biosurfactant causes the haemolysis of human erythrocytes by a colloid-osmotic mechanism, most likely by the formation of enhanced permeability domains. Our results suggest that the mechanism of action of rhamnolipids is complex and that other factors may be involved in the haemolysis. When comparing the results of characterization of the aggregates formed with haemolysis results it can be stated that the size and rigidity of the aggregate can play an important role in the haemolytic behaviour of rhamnolipids, the bigger the aggregate size and rigidity, the smaller the haemolytic activity. Similar results were obtained for gemini surfactants [37].

3.6. Vesicle permeation studies

The presence of surfactants has a strong influence on the permeability of vesicle bilayer membrane [38]. Since rhamnolipids are anionic surfactants it is expected that the presence of these compounds strongly influences the properties of the vesicles. In the present study, the rate of CF release from DPPC and RL/DPPC mixed vesicles was measured to assess the influence of rhamnolipids in the permeability of the vesicles. For DPPC vesicles, after 10 min the fluorescence starts to increase slowly with time, reaching a constant value of 40% release after 30 min. Vesicles containing the rhamnolipid immediately produce a fluorescence profile comparable to that of 100% release, therefore it was not possible to take measurements as a function of time. The presence of the rhamnolipids increases the bilayer fluidity, possibly by defect creation. As a consequence, mixed vesicles are more permeable for the encapsulated dye.

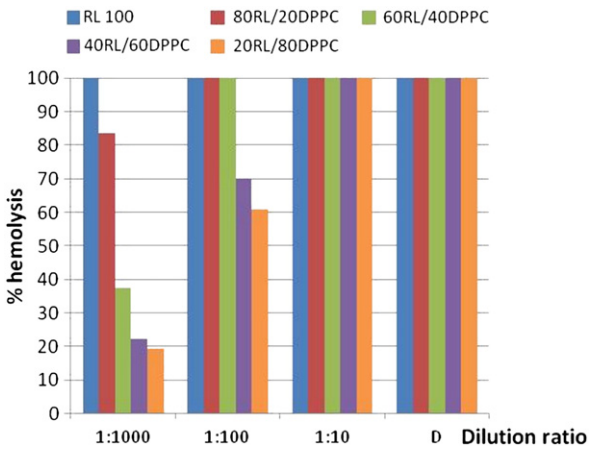

Fig. 9. Haemolysis values produced when pure RL8 and four RL8/DPPC mixtures are exposed to human erythrocytes. D: Each one of the 0.14% (W/W) solutions is tested directly. 1:10, 1:100 and 1:1000 are subsequent dilutions from D.

To correlate the haemolytic activity with the interaction ability of rhamnolipids with DPPC vesicles, an additional test was carried out. For this test DPPC and rhamnolipid vesicle dispersions of the same concentration were prepared separately. Then the release of the CF on the DPPC vesicles was measured for 30 min. After this time 60 μl of rhamnolipid vesicle dispersion was added. The fluorescence intensity increased immediately, reaching a value similar to that achieved by adding Triton X-100. This result is parallel to the strong haemolytic activity observed for rhamnolipid dilutions smaller than 1:100 in Fig. 9.

4. Conclusions

Both RH and DPPC form bilayers which can form vesicles. The mixtures have zeta-potential and sizes that do not differ dramatically with that of the pure components, except for the z-potential of DPPC vesicles in acidic media, which is positive, compared with the results obtained for the rest of the samples, which have a negative zeta-potential from −20 mV to −40 mV. The biosurfactant forms ordered bilayers with long repeating distances; these long repeating distances are stabilized by the charging of the bilayer and also by a strong fluidity of the bilayers. The ability of RL8 to increase the fluidity of DPPC bilayers is parallel to the increase of vesicle permeation and may be related with the strong haemolytic power of these molecules.

Acknowledgements

We thank Jaume Caelles from the SAXS-WAXS service at IQAC for the X-ray measurements. Financial support from MINECO CTQ2010-14897 and MAT2012-38047-CO2-02 is gratefully acknowledged. Also financial support from Generalitat de Catalunya 2009SGR1331 is gratefully acknowledged.

References

[1] V.A. Pashynska, Mass spectrometric study of rhamnolipid biosurfactants and their interactions with cell membrane phospholipids, Biopolym. Cell 25 (2009) 504–508.
[2] M. Sanchez, F.J. Aranda, M.J. Espuny, A. Marques, J.A. Teruel, A. Manresa, A. Ortiz, Aggregation behaviour of a dirhamnolipid biosurfactant secreted by *Pseudomonas aeruginosa* in aqueous media, J. Colloid Interface Sci. 307 (2007) 246–253.
[3] J. Penfold, R.K. Thomas, H. Shen, Adsorption and self-assembly of biosurfactants studied by neutron reflectivity and small angle neutron scattering: glycolipids, lipopeptides and proteins, Soft Matter 8 (2012) 578–591.
[4] P. Fernandez, N. Willenbacher, T. Frechen, A. Kühnle, Vesicles as rheology modifier, Colloids Surf. A: Physicochem. Eng. Aspect 262 (2005) 204–210.
[5] D. Paolino, D. Cosco, R. Muzzalupo, E. Trapasso, N. Picci, M. Fresta, Innovative bola-surfactant niosomes as topical delivery systems of 5-fluorouracil for the treatment of skin cancer, Int. J. Pharm. 353 (2008) 233–242.
[6] P. Balakrishnan, S. Shanmugam, W.S. Lee, W.M. Lee, J.O. Kim, D.H. Oh, D. Kim, J.S. Kim, B.K. Yoo, H. Choi, J.S. Woo, C.S. Yong, Formulation and in vitro assessment of minoxidil niosomes for enhanced skin delivery, Int. J. Pharm. 377 (2009) 1–8.
[7] A.C.S. Lawrence, Solubility in soap solutions. 10. Phase equilibrium, structural and diffusion phenomena involving the ternary liquid crystalline phase, Discuss. Faraday Soc. 25 (1958) 51–58.
[8] A.D. Bangham, M.M. Standish, J.C. Watkins, Diffusion of univalent ions across lamellae of swollen phospholipids, J. Mol. Biol. 13 (1965) 238–252.
[9] D. Orthaber, A. Bergmann, O. Glatter, SAXS experiments on absolute scale with Kratky systems using water as a secondary standard, J. Appl. Crystallogr. 33 (2000) 218–225.
[10] L. Pérez, A. Pinazo, M.R. Infante, R. Pons, An investigation of the micellization process of single and gemini surfactants from arginine by SAXS, NMR self-diffusion, and light scattering, J. Phys. Chem. B 111 (2007) 11379–11387.
[11] J. Morros, M.R. Infante, R. Pons, Surface activity and aggregation of pristine and hydrophobically modified inulin, Soft Matter 8 (2012) 11353–11362.
[12] G. Pabst, M. Rappolt, H. Amenitsch, P. Laggner, Structural information from multilamellar liposomes at full hydration: full q-range fitting with high quality X-ray data, Phys. Rev. E Stat. Phys. Plasmas Fluids Relat. Interdiscip. Top. 62 (2000) 4000–4009.
[13] G. Rodríguez, M. Cócera, L. Rubio, C. Alonso, R. Pons, C. Sandt, P. Dumas, C. López-Iglesias, A. de la Maza, O. López, Bicellar systems to modify the phase behaviour of skin stratum corneum lipids, Phys. Chem. Chem. Phys. 14 (2012) 14523–14533.
[14] A. Zaragoza, F.J. Aranda, M.J. Espuny, J.A. Teruel, A. Marques, A. Manresa, A. Ortiz, Hemolytic activity of a bacterial trehalose lipid biosurfactant produced by *Rhodococcus* sp.: evidence for a colloid-osmotic mechanism, Langmuir 26 (2010) 8567–8572.
[15] J.N. Weinstein, S. Yoshikami, P. Henkard, R. Blumenthal, W.A. Hagins, Liposome–cell interaction: transfer and intracellular release of a trapped fluorescent marker, Science 195 (1977) 489–492.
[16] A. Abalos, A. Pinazo, R. Infante, M. Casals, F. García, A. Manresa, Physicochemical and antimicrobial properties of new rhamnolipids produced by *Pseudomonas aeruginosa* AT10 from soybean oil refinery wastes, Langmuir 17 (2001) 1367–1371.
[17] C. Syldatk, C.F. Wagner, Production of Biosurfactants, in: N. Kosaric, W.L. Cairns (Eds.), Biosurfactants and Biotechnology, Marcel Dekker, New York, 1987.
[18] E. Haba, A. Pinazo, O. Jauregui, M.J. Espuny, M.R. Infante, A. Manresa, Physicochemical characterization and antimicrobial properties of rhamnolipids produced by *Pseudomonas aeruginosa* 47T2 NCBIM 40044, Biotechnol. Bioeng. 81 (2003) 316–322.
[19] M. Benincasa, A. Abalos, I. Oliveira, A. Manresa, Chemical structure, surface properties and biological activities of the biosurfactant produced by *Pseudomonas aeruginosa* LBI from soapstock, Antonie Van Leeuwenhoek 85 (2004) 1–8.
[20] F.B. Rosevear, Liquid crystals: the mesomorphic phases of surfactants, J. Soc. Cosmet. Chem. 19 (1968) 581–594.
[21] A. Lebron-Paler, J.E. Pemberton, B.A. Becker, W.H. Otto, C.K. Larive, R.M. Maier, Determination of the acid dissociation constant of the biosurfactant monorhamnolipid in aqueous solution by potentiometric and spectroscopic methods, Anal. Chem. 78 (2006) 7649–7658.
[22] M. Chen, J. Penfold, R.K. Thomas, T.J.P. Smyth, A. Perfumo, R. Marchant, I.M. Banat, P. Stevenson, A. Parry, I. Tucker, I. Grillo, Solution self-assembly and adsorption at the air–water interface of the monorhamnose and dirhamnose rhamnolipids and their mixtures, Langmuir 26 (2010) 18281–18292.
[23] S.H. Kim, Y. Park, S. Matalon, E.I. Franses, Effect of buffer composition and preparation protocol on the dispersion stability and interfacial behavior of aqueous DPPC dispersions, Colloids Surf. B: Biointerfaces 67 (2008) 253–260.
[24] O. Pornsunthorntawee, S. Chavadej, R. Rujiravanit, Solution properties and vesicle formation of rhamnolipid biosurfactants produced by *Pseudomonas aeruginosa* SP4, Colloids Surf. B 72 (2009) 6–15.
[25] O. López, M. Cócera, R. Pons, N. Azemar, A. de la Maza, Kinetic studies of liposome solubilization by sodium dodecyl sulfate based on a dynamic light scattering technique, Langmuir 14 (1998) 4671–4674.
[26] N. Lozano, A. Pinazo, C. La Mesa, L. Perez, P. Andreozzi, R. Pons, Catanionic vesicles formed with arginine-based surfactants and 1,2-dipalmitoyl-sn-glycero-3-phosphate monosodium salt, J. Phys. Chem. B 113 (2009) 6321–6327.
[27] K. Makino, T. Yamada, M. Kimura, T. Oka, H. Ohshima, T. Kondo, Temperature- and ionic strength-induced conformational changes in the lipid head group region of liposomes as suggested by zeta potential data, Biophys. Chem. 41 (1991) 175–183.
[28] D.H. Mengistu, E.E. Kooijman, S. May, Ionization properties of mixed lipid membranes: a Gouy–Chapman model of the electrostatic–hydrogen bond switch, Biochim. Biophys. Acta Biomembr. 1808 (2011) 1985–1992.
[29] J.T. Champion, J.C. Gilkey, H. Lamparski, J. Retterer, R.M. Miller, Electron microscopy of rhamnolipid (biosurfactant) morphology: effects of pH, cadmium and octane, J. Colloid Interface Sci. 170 (1995) 569–574.
[30] B. Dahrazma, C.N. Mulligan, M.P. Nieh, Effects of additives on the structure of rhamnolipid (biosurfactant): a small-angle neutron scattering (SANS) study, J. Colloid Interface Sci. 319 (2008) 590–593.
[31] A. Ortiz, J.A. Teruel, M.J. Espuny, A. Marques, A. Manresa, F.J. Aranda, Effects of dirhamnolipid on the structural properties of phosphatidylcholine membranes, Int. J. Pharm. 325 (2006) 99–107.
[32] T. Lenne, C.J. Garvey, K.L. Koster, G. Bryant, Effects of sugars on lipid bilayers during dehydration — SAXS/WAXS measurements and quantitative model, J. Phys. Chem. B 113 (2009) 2486–2491.
[33] E.G. Finer, M.C. Phillips, Factors affecting molecular packing in mixed lipid monolayers and bilayers, Chem. Phys. Lipids 10 (1973) 237–252.
[34] T. de Paula Rigoletto, M.E.D. Zaniquelli, M.H.A. Santana, L.G. de la Torre, Surface miscibility of EPC/DOTAP/DOPE in binary and ternary mixed monolayers, Colloids Surf. B: Biointerfaces 83 (2011) 260–269.
[35] A. Colomer, A. Pinazo, M.T. García, M. Mitjans, M.P. Vinardell, M.R. Infante, V. Martínez, L. Pérez, pH-sensitive surfactants from lysine: assessment of their cytotoxicity and environmental behavior, Langmuir 28 (2012) 5900–5912.
[36] M. Sanchez, F.J. Aranda, J.A. Teruel, M.J. Espuny, A. Marques, A. Manresa, A. Ortiz, Permeabilization of biological and artificial membranes by a bacterial dirhamnolipid produced by *Pseudomonas aeruginosa*, J. Colloid Interface Sci. 341 (2010) 240–247.
[37] L. Tavano, M.R. Infante, M.A. Riya, A. Pinazo, M.P. Vinardell, M. Mitjans, M.A. Manresa, L. Perez, Role of aggregate size in the hemolytic and antimicrobial activity of colloidal solutions based on single and gemini surfactants from arginine, Soft Matter 9 (2013) 306–319.
[38] S. Bhattacharya, S. Haldar, Synthesis, thermotropic behavior, and permeability properties of vesicular membranes composed of cationic mixed-chain surfactants, Langmuir 11 (1995) 4748–4757.